Individualized Biokinetic modelling of Iodine-131 in thyroid cancer treatments: implications on internal dosimetry

Jacobo Guiu-Souto[1*], Sara Neira-Castro[1], Manuel Sánchez-García[1], Oscar López-Pouso[2], Miguel Pombar-Cameán[1,3] and Juan Pardo-Montero[1,3]

[1] Department of Medical Physics and Radiological Protection. University Hospital of Santiago de Compostela. Spain.
[2] Department of Applied Mathematics. University of Santiago de Compostela. Spain.
[3] Molecular Imaging Group, IDIS Health Research Institute, Santiago de Compostela. Spain.

*E-mail: jacobo.guiu.souto@sergas.es

Abstract

Nowadays therapies involving radioiodine (I-131) represents the 84% of the total metabolic treatments in Europe, according to the last report of European Association of Nuclear Medicine (EANM) in relation to treatment planning for molecular radiotherapy. Last recommendations of the European Council, i.e. 2013/59/Euroatom, mandates that metabolic treatments should be planned according to the radiation doses delivered to individual patients, analogous to the external beam radiotherapy. In this work, we present a novel biokinetic model for I-131 that allows to obtain realistic activity distributions for particular patients. Other models existing in the literature are either rather simple to obtain realistic results or too complex for adjusting to individual patients. The individualization of activity distribution is overcoming by an optimization method that adjusts our model to a set of experimental measurements. Significant differences in terms of absorbed doses are observed between our model and the standard generalist models, especially in terms of red marrow absorbed dose.

1. Introduction

Thyroid cancer presents a incidence rate of 10/10000 [1] and it has been increasing over the last decades [2, 3], even if the trends are maintained this cancer might became one of the most common in the United States [4]. Radioiodine I-131 is the gold standard for treating patients with well-differentiated thyroid cancer (DTC). To date the main approach to this therapy is still based on administering fixed activities, which in certain cases may depend on the patient weight [5]. Last method does not allow to know doses to tumor and organs at risks. In particular when recurrences take place high activities are delivered so determining red-marrow absorbed dose is crucial. A better option is the use of generalist biokinetic models that are the base for dosimetric calculations. However, generalist models are not useful to obtain an individualized dosimetry since each patient presents its particular metabolism.

During last decades absorbed-dose estimations have undergone major progresses than biokinetic models, going from standard hermaphrodite adult phantoms [6, 7] to a more realistic ones, i. e. anthropomorphic/deformable phantoms [8-11], or even, analogous to external

radiotherapy, computing on the real patient anatomy by computed tomography [12]. Thus, the challenge is not to improve the dosimetric calculations but achieving more realistic and individualized biokinetic models to known the real activity distribution of patients.

The biokinetic distribution of iodide has been studied extensively and there are several models trying to describe its behaviour [13-17]. The model presented by the International Commission on radiological protection (ICRP) in Publication 53 [18] presents a simplified kinetic and therefore great imprecisions on dose calculations. Otherwise, ICRP in its Publication 128 [19] presented a more complex model that describes iodine metabolisms in high detail, using a great number of interconnected compartments that makes a difficult task adjusting the model to the individual biokinetics of patients. Furthermore, sometimes these models are not indicated for patients receiving therapeutic amounts of radioiodine, since it might affect iodine metabolism, as occurs in the model reported by the Medical Internal Radiation Commission (MIRD) in its dose estimate report No. 5 [14].

The European directive 2013/59/Euratom [20] mandates that all medical exposures of patients for radiotherapic purposes, including nuclear medicine therapies (here on metabolic radiotherapy), shall indicate exposures of target volumes and organs at risk individually. Moreover, non-target volumes shall receive doses as low as reasonably achievable. It is important to note that treatment outcome is dependent on the absorbed doses to tumor not on the administered activity. According to the last report of the European Association of Nuclear Medicine (EAMN) about Internal Dosimetry [5], therapies involving I-131 represents 84% of treatment patients and the 71% of the metabolic treatments, and despite that, in the most of cases medical physicist are not involved, and therefore, absorbed dose planning was never carried out. To date, in treatment of DTC there are no well-established values for absorbed doses to remnants which may be used as prescription values but the treatment is performed by administration of a fixed activity depending on the stage of the disease.

Thus, it is necessary to develop more precise biokinetic models that allow to apply an individual internal dosimetry for each treatment. In this work, we present a biokinetic model midway between ICRP 53 and ICRP 128 models. The advantage of our model is that presents a well-description of radioiodine biokinetics at the same time that its low complexity allows to adjust to each patient. The calculation of the individualized activity distribution is overcoming by an optimization method that adjusts our model to a set of experimental measurements. A group of different patients is analysed and compared to the above generalist biokinetics models and to other standard empiric models for red marrow dosimetry [21, 22].

The structure of the manuscript is the following. In Section 2 we describe the biokinetic model, the optimization methods and the experimental data. In the next Section we show the results of the comparison between our model and other generalists/empiric models. Finally, in Section 4 we present the conclusions of the work.

2. Materials and methods

2.1. Model description and dosimetry calculations

The model here presented (see Fig. 1a) evolves from the ICRP Publication 53. To adapt this model to the treatment of DTC we have added more compartments. First, as the iodine I-131 is applied by oral administration, we use the compartments corresponding to the human alimentary tract model [23], i.e.: stomach, small intestine, large intestine, bladder and body fluid. At this point, according to recent literature [19] we introduce a feedback between body fluid and stomach. We also include a compartment to model the remaining thyroid tissue post thyroidectomy. Organic and inorganic iodine are located in separated pools, i.e. organic pool and body fluids, respectively. Finally, in liver takes place the deiodination of thyroid hormones

returning part of the iodine to the body fluids in its inorganic form. As it is shown in Figure 1b the main organs appearing in the scintigraphy are included in the model. Only salivary glands are not considered due to experimental limitations on data acquisition.

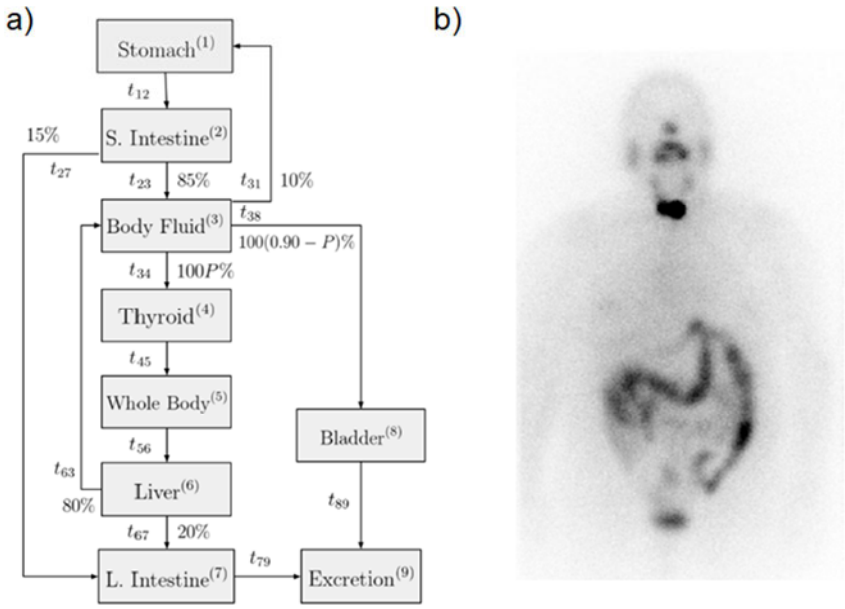

Figure 1. a) Scheme of our compartment model for I-131 biokinetics. t_{ij} refers to the half-time coefficients between compartments. b) Illustrative planar scintigraphy 24 hours post administration of 100 mCi of I-131.

The model constitutes the following system of coupled ordinary differential equations:

$$\frac{dA_j(t)}{dt} = (k_{jj} - \lambda)A_j + \sum_{i \neq j} k_{ij} A_i(t) \quad (1)$$

where A_j is the activity of compartment j and $k_{ij} = \ln(2)/t_{ij}$ the rate constants with t_{ij} as the half-time coefficients between compartments i and j. Starting values of the rate constants for the optimization method are presented in Table 1. These values are obtained from generalist biokinetic models [14-19]. To solve the model we use a four order Runge-Kutta method with a variable temporal step [24]. As an initial condition we consider the administered activity (A_0) at stomach and zero the rest of compartments. To obtain the cumulated activity we use the integration method of Simpson [25].

The absorbed doses are calculated from cumulated activity by applying specific absorbed fractions based on anthropomorphic phantoms [7]. We compare our results to the different generalist models, ICRP 53, MIRD 5 and ICRP 128, considering the lowest tabulated uptake value, usually a 5 %.

2.2. Optimization and numerical methods

Against to the generalist models in this work we perform an optimization method to adjust the rate constants to the particular biokinetics of each patient. The objective function corresponds to the chi-square of the difference between theoretical and experimental activities for a set of compartments (C) and times (N):

$$m(t_{ij}) = \min\left\{\sum_{k=1}^{C}\left(\sum_{n=1}^{N}\left(A^k(t_n) - X^k(t_n)\right)^2\right)\right\} \quad (2)$$

where *A(t)* and *X(t)* represent the value of theoretical and experimental activities for a given time, n, respectively. Due to the high number of rate constants involved in the optimization, a "brute-force" simulation is not indicated. Thus to minimize objective function we varied rate constants by an annealing algorithm [26]. On each iteration of the optimization method the algorithm solves the model equations with a set of rate constants perturbed randomly and evaluated the objective function. The optimal solution is that presents the minimum value of the objective function.

Out-Compartment	In-Compartment	Half-time	Rate Constant*)
Stomach (1)	Small Intestine (2)	t12 = 3 h	k12 = 0.23
Small Intestine (2)**)	Body Fluid (3)	t23 = 5 h	k23 = 0.14
Small Intestine (2)**)	Low Intestine (7)	t27 = 5 h	k27 = 0.14
Body Fluid (3)	Stomach (1)	t31 = 0.34 h	k31 = 2.04
Body Fluid (3)	Thyroid (4)	t34 = 6 h	k34 = 0.12
Body Fluid (3)	Bladder (8)	t38 = 6 h	k38 = 0.12
Thyroid (4)	Whole Body (5)	t45 = 20 d	k45 = 0.03
Whole body (5)	Liver (6)	t56 = 8	k56 = 0.09
Liver (6)	Low intestine (7)	t67 = 10	k67 = 0.07
Liver (6)	Body Fluid (3)	t63 = 10	k63 = 0.07
Low intestine (7)	Exterior (9)	t79 = 24 h	k79 = 0.03
Bladder (8)	Exterior (9)	t89 = 8 h	k89=0.09

*) k=ln2/t

**) branching ratios: (2) → (3) [85%], (2) → (7) [15%], (6) → (7) [20%] and (6) → (3) [80%]

Table 1 Starting values of rate constants for biokinetic model of Figure 1. Rate constants are expressed in terms of half-time turnover.

2.3. Experimental data

The estimation of activities on whole body (WB) and remaining thyroid tissue (RTT) were carried out by a scintillation detector (Exploranium GR-130 Radiation Spectrometer Scintillation Detector). We measure the exposition (μGy/h), along 10 temporal points, after the administration of the radioiodine. The detector was placed at different locations: at 2 m in front of patient for WB and at neck contacting to thyroid. Only patients with RTT (after thyroidectomy) at neck, in absence of any metastasis, are considered in this study.

A calibration coefficient (19.2 ± 1.2 μSv/kBq) that converts dose values of the detector into activity was obtained by using two flood phantoms (length/radius: 10 cm/5 cm and 30 cm/15 cm) calibrated with 2 mCi of I-131. Small phantom represents the remainders and calibration is performed by contacting, while the other for whole body purposes is located at 2 m far from the detector. Moreover, these phantoms allow us to evaluate the constancy of detector readouts along the experiment. In addition, we compare the WB coefficient with the corresponding measurement taken just after the oral administration of the I-131 when all activity still remains inside of patient, i.e.: 18.1 ± 1.1 μSv/kBq. We observed that both values are in good agreement.

A set of 6 blood samples are taken following a similar schedule used in whole body measurements. Samples of 1 ml are collected in test tubes and analysed by a contamination monitor (Berthold LB 124 SCINT). A conversion factor of 0.33 ± 0.05 cpm/kBq (**consular valor con Manuel**) is determined by an initial measurement of the test tube calibrated with 1

mCi of I-131(**consular valor con Manuel**). Finally, by estimating the blood volume of the patient, from the Nalder´s formula [27], we obtain the total activity in this compartment.

We analysed 20 patients with well-differentiated thyroid cancer: 15 females with a mean age of 49 (ranging from 34 to 78) and weight of 74 ± 12 kg, and 5 males with a mean age of 49 (ranging from 40 to 55) and a weight of 90 ± 18 kg. Selected patients present papillar or follicular thyroid cancer types and total thyroidectomy. The remaining thyroid tissue was treated by oral administration with 100 mCi of I-131 after a regimen of iodine suspension for 3 weeks.

3. Results and discussion

In Figure 2 it is shown the activity on the compartments of the model for an individual patient. Experimental measurements are also included in the figure for RTT, whole body and body fluids. The evolution of the total activity contained in the patient presents an exponential decay, with resident time of 26.2 h. At 30 hours from the administration it is excreted the 80 % of the iodine mainly by urine. The principal contribution to the total activity after 90 hours is due to the RTT. Body fluids presents a biexponential behaviour with a resident time of $9.2 \cdot 10^{-4}$ h per millilitre**.** The peak of Body Fluids curve takes place at 5 hours, the intake rate is faster respect to bladder transference. RTT compartment reaches the maximum uptake after 27 hours from the administration with a value 4.7 %. Afterwards the kinetics of the compartment is fundamentally controlled by the iodine decay. The model fits to experimental data in a good agreement.

Red marrow dosimetry is obtained by applying absorbed-dose coefficients (S-factors), [7] to the cumulated activity derived from Figure 2. The equivalent dose at RM results 280 mGy. This value is in agreement to the obtained by other empiric methods, as the EAMN [28, 29] with a value of 465.8 mGy, and the Italian Association of Physics in Medicine (AIFM) with a value of and 335.6 mGy [30, 31]. EANM approach evaluates the absorbed dose to blood, assuming that is the same as RM, analogous to Benua's work. AIMF estimates directly dose to RM, it is based on the linear scaling of S-factors with the mass of patient and the assumption of the activity concentrations of blood and RM are identical in metabolic radiotherapy.

Due to the optimization method is based in a simulating annealing technique the solution of the model present an inherent degeneration. This degeneration is quantified by performed a set of repeated simulations, preserving identical initial conditions and same experimental inputs as Fig.2. In Table 2, we show the influence on the dosimetry of including different experimental data to the optimization method. We observed that by using only one compartment, as total activity, the degeneration of the model is elevate. The normalized interval of degeneration, C_1, is the order of the median. RTT presents variations from 22.6 mGy/MBq to 58.1 mGy/MBq and RM ranging from 0.022 mGy/MBq to 0.034 mGy/MBq. Thus one-compartment optimization is not suitable for perform an individualized dosimetry.

However, by adding more experimental data to the optimization, as body fluids and RTT, the degeneration is reduced significantly. The normalized interval of degeneration, C_3, is reduced around 80% with respect to C_1. One of the major reductions is achieved for RTT, which is an expected result due to the relation of this compartment with the experimental inputs. Other important reduction takes place in bladder, it is due to the relation between bladder and body fluids (see fig. 1) which is measured experimentally.

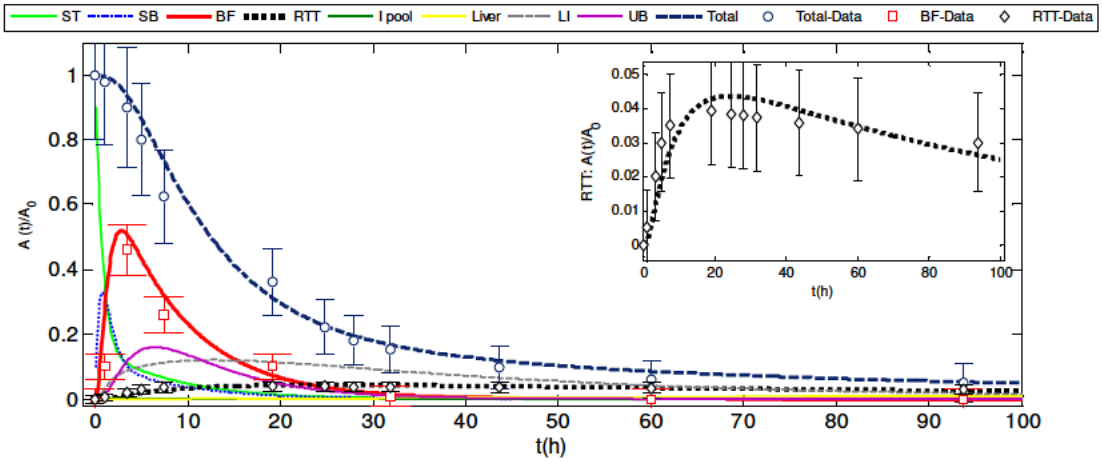

Figure 2. (Colour online) A(t)/A0 is the normalized activity (A0 = 3.7 GBq) of each compartment of SdC model versus time (hours). "ST" denotes stomach, "SB" small bowel, "BF body fluid", "RRT" remaining thyroid tissue, "I pool" organic iodine pool, "LI" Large intestine, "UB" bladder, "Total" is the sum of the activity in all compartments and "Data" refers to experimental measurements.

	1-COMPART. OPTIMIZATION					3-COMPARTS. OPTIMIZATION					R (%)
Organs	**Mean**	**D1**	**D5**	**D9**	**C_1**	**Mean**	**D1**	**D5**	**D9**	**C_3**	
LLI	1.755	0.554	1.687	3.214	1.58	2.827	2.512	2.807	3.188	0.24	84.7%
SI	0.101	0.053	0.101	0.151	0.97	0.108	0.102	0.108	0.118	0.15	84.2%
Stomach	0.642	0.291	0.454	1.393	2.42	0.635	0.421	0.645	0.886	0.72	70.3%
ULI	0.040	0.029	0.042	0.054	0.59	0.047	0.045	0.047	0.052	0.16	73.7%
Kidneys	0.018	0.012	0.015	0.030	1.18	0.019	0.017	0.019	0.022	0.29	75.5%
Liver	0.038	0.022	0.040	0.050	0.70	0.028	0.030	0.025	0.038	0.33	52.7%
Lungs'	0.017	0.011	0.016	0.025	0.84	0.013	0.012	0.013	0.014	0.15	82.1%
RM	0.027	0.022	0.027	0.034	0.44	0.031	0.029	0.031	0.032	0.10	77.1%
RTT	42.93	22.61	46.62	58.11	0.76	28.14	27.10	28.67	29.15	0.07	90.4%
Bladder	1.568	0.081	2.006	2.904	1.41	1.701	1.616	1.712	1.750	0.08	94.4%
WB	0.047	0.044	0.046	0.050	0.12	0.045	0.044	0.045	0.046	0.04	68.3%

Table 2 Degeneration of the model in terms mGy/MBq for certain organs. Number of performed simulations: 50. D1, D5 and D9 are first decil, median and ninth decil, respectively. $C_{1,2}$ = (D9-D1)/D5 represents the degeneration interval normalized by median. R = 1 – C_3/C_1, represents the reduction of the degeneration. L(U)LI – Lower (Upper) Large Intestine, SI – Small Intestine, RM – Red Marrow, RTT – Remaining Thyroid Tissue and WB- Whole Body.

In figure 3 we present a comparison between generalist models, as ICRP 53, MIRD 5 or ICRP 128, and our model for a set of patients. Firstly, we observed that differences between patients are considerable and generalist models present difficulties to describe each individual biokinetics. MIRD 5 model underestimates doses for all set of patients. Equivalent dose per unit of activity at stomach ranges from 0.02 mGy/MBq to 0.14 mGy/MBq. The median of the patients distribution is 0.51 mGy/MBq which is in agreement to both ICRP models. In liver equivalent doses per unit of activity goes from 0.015 mGy/MBq to 1.4 mGy/MBq with a median in relation to ICRP predictions with a value of 0.05 mGy/MBq. The distribution of equivalent dose at lung ranges from 0.007 mGy/MBq to 0.05 mGy/MBq. In this case the median of patients distribution, i.e.: 0.017 mGy/MBq, is lower than both ICRP models. RTT present values in the interval from 13.1 mGy/MBq to 72 mGy/MBq with a median of 34.9 mGy/MBq. Generalist models are based on standard uptake values and for this reason their predictions result less accurate.

For patients considered in this study, i.e. treated with 3.7 GBq, the median value of equivalent dose to RM results 133 mGy, and the highest value is 518 mGy. Last values are far from the dose constrain of 200 cGy related to red marrow depression [32, 33]. According to this, the maximum permissible activity, estimated from this maximum value, is 14.2 GBq which is in agreement to the results of Miranti *et al.*

Finally, effective dose for patients goes from 4.1 mSv to 10.4 mSv. In this case our values are in the interval defined between ICRP 53 and ICRP 128.

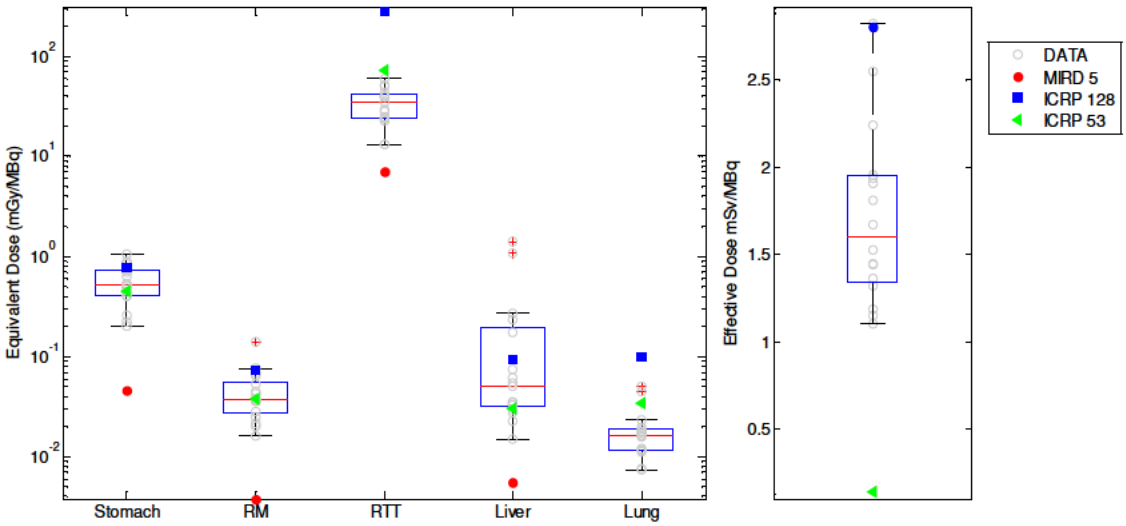

Figure 3. Comparison between generalist models (ICRP 53, MIRD 5 and ICRP 128) and our model. Number of analysed patients: 20. Left: equivalent doses (mGy/MBq) for a set of compartments: stomach, red marrow (RM), remaining thyroid tissue (RTT), liver and lung. Right: effective dose (mSv/MBq). "Empty circles" correspond to model estimations, "filled circles" to MIRD 5, "filled squares" to ICRP 128 and "filled triangles" to ICRP 53. On each box, the central mark indicates the median, and the bottom and top edges of the box indicate the 25th and 75th percentiles, respectively. The whiskers extend to the most extreme data points.

4. Conclusions

In this work we present a novel biokinetic model with a complexity degree, midway between ICRP 53 and ICRP 128, that allows to perform individualized dosimetry in a realistic way. To adjust our model to the biokinetics of patients we develop an optimization method based on the simulated annealing method. Inherent degeneration of the model solution is reduced significantly by including different experimental measurements (RTT, blood samples and whole body). We observe that performing only one compartment optimization is insufficient for the aim of individualized dosimetry. The model fits experimental data in good agreement. The estimations of equivalent dose at red marrow are similar to other empiric models based in blood samples and whole body measurements [21, 22].

A set of patients were analysed and compared to the generalist models from both ICRP and MIRD. We find significant differences between dose distributions of patients obtained with our model and the generalist predictions. At red marrow level we obtain dose values much lower to the limit of 200 cGy and the estimations of the permissible activities are in relation to the literature [21, 22]. Moreover, the determination of equivalent dose to remaining thyroid tissues is crucial to perform future dose-effect studies.

To conclude, the authors want to remark that the number of radiopharmaceuticals and their applications have expended significantly and the methods addressed in this manuscript can be applied to other novel metabolic treatments.

Acknowledgements

J. P-M is supported by ISCIII through a Miguel Servet grant (CP12/03162).

References

[1] Vecchia C, Malvezzi M, Bosetti C, Garavello W, Bertuccio P, Levi F and Negri E Thyroid cancer mortality and incidence: A global overview Int. J. Cancer: 136, 2187–2195 (2015)

[2] Davies L, Welch HG. Increasing incidence of thyroid cancer in the United States, 1973–2002. JAMA 2006; 295:2164–7.

[3] Horn-Ross PL, Lichtensztajn DY, Clarke CA, et al. Continued rapid increase in thyroid cancer incidence in California: trends by patient, tumor and neighborhood characteristics. Cancer Epidemiol Biomarkers Prev 2014;23: 1067–79.

[4] Rahib L, Smith BD, Aizenberg R, et al. Projecting cancer incidence and deaths to 2030: the unexpected burden of thyroid, liver, and pancreas cancers in the United States. Cancer Res 2014;74: 2913–21.

[5] Report EANM

[6] Snyder W, Ford M, Warner G: Estimates of Specific Absorbed Fractions for Photon Sources Uniformly Distributed in Various Organs of a Heterogeneous Phantom [MIRD Pamphlet No. 5 (revised)], New York, 1978, Society of Nuclear Medicine.

[7] Cristy M, Eckerman K: Specific Absorbed Fractions of Energy at Various Ages from Internal Photon Sources (ORNL Report ORNL/TM-8381 V1-V7), Oak Ridge, TN, 1987, Oak Ridge National Laboratory.

[8] Stabin MG1, Emmons MA, Segars WP, Fernald MJ. Realistic reference adult and paediatric phantom series for internal and external dosimetry Radiat Prot Dosimetry. 2012 Mar;149(1):56-9.

[9] Yong Hum Na,1 Binquan Zhang,2 Juying Zhang,2 Peter F Caracappa,2 and X George Xu1,2 Deformable adult human phantoms for radiation protection dosimetry: anthropometric data representing size distributions of adult worker populations and software algorithms Phys Med Biol. 2010 Jul 7; 55(13): 3789–3811.

[10] Segars J. P. The University of North Carolina; 2001. Development and application of the new dynamic NURBS-based cardiac-torso (NCAT) phantom. Ph.D. dissertation

[11] Susan Kost, Michael Stabin1 and William Segars Patient-specific dosimetry based on deformable anthropomorphic models J Nucl Med May 2013 vol. 54 no. supplement 2 49

[12] Xie George Xu and Keith F. Ecckerman Handbook of anatomical models for radiation dosimetry Taylor & Francis Group 2009.

[13] Riggs, D.S., 1952. Quantitative aspects of iodine metabolism in man. Pharmacol. Rev. 4, 284–370.

[14] MIRD Dose Estimate Report No. 5. Summary of current radiation dose estimates to humans for I-123, I-124, I-125, I-126, I-130, I-131 as sodium iodide J Nucl. Med. 1975; 16:857-860.

[15] Johansson, L., Leide-Svegborn, S., Mattsson, S., et al., 2003. Biokinetics of iodide in man: refinement of current ICRP dosimetry models. Cancer Biother. Radiopharm. 18, 445–450.

[16] Leggett, R.W., 2010. A physiological systems model for iodine for use in radiation protection. Radiat. Res. 174, 496–516.

[17] Leggett, R.W., 2017. An age-specific biokinetic model for iodine. J Radiol Prot 37(4) 864-882.

[18] ICRP, 1988. Radiation dose to patients from radiopharmaceuticals. ICRP Publication 53. Ann. ICRP 18(1-4).

[19] ICRP, 2015. Radiation Dose to Patients fromRadiopharmaceuticals: A Compendium of Current Information Related to Frequently Used Substances. ICRP Publication 128. Ann. ICRP 44(2S).

[20] COUNCIL DIRECTIVE 2013/59/EURATOM of 5 December 2013 laying down basic safety standards for protection against the dangers arising from exposure to ionising radiation, and repealing Directives 89/618/Euratom, 90/641/Euratom, 96/29/Euratom, 97/43/Euratom and 2003/122/Euratom. 2014, Official Journal of the European Union.

[21] A Giostra, E Richetta, M Pasquino, A Miranti, C Cutaia, G Brusasco, R E Pellerito and M Stasi Red marrow and blood dosimetry in 131I treatment of metastatic thyroid carcinoma: pre-treatment versus in-therapy results Phys. Med. Biol. 61 (2016) 4316–4326

[22] A Miranti, A Giostra, E Richetta, E Gino, R E Pellerito and M Stasi Comparison of mathematical models for red marrow and blood absorbed dose estimation in the radioiodine treatment of advanced differentiated thyroid carcinoma Phys. Med. Biol. 60 (2015) 1141–1157

[23] ICRP, 2006. Human alimentary tract model for radiological protection. ICRP Publication 100. Ann ICRP. 2006; 36(1-2):25-327

[24] Runge Kutta

[25] Integration method of Simpson

[26] Annealling

[27] Nadler SB, Hidalgo JH, Bloch T. Prediction of blood volume in normal human adults. surgery. 1962 Feb;51(2):224-32.

[28] Lassmann M, Hänscheid H, Chiesa C, Hindorf C, Flux G and Luster M 2008 EANM dosimetry Committee series on standard operational procedures for pre-therapeutic dosimetry: I. Blood and bone marrow dosimetry in differentiated thyroid cancer therapy Eur. J. Nucl. Med. Mol. Imag. 35 1405–12

[29] Hindorf C, Glatting G, Chiesa C, Lindén O and Flux G 2010 EANM Dosimetry Committee guidelines for bone marrow and whole-body dosimetry Eur. J. Nucl. Med. Mol. Imag. 37 1238–50

[30] Stabin M G and Siegel J A 2003 Physical models and dose factors for use in internal dose assessment Health Phys. 85 294–310

[31] Chiesa C et al 2009 Individualized dosimetry in the management of metastatic differentiated thyroid cancer Q. J. Nucl. Med. Mol. Imaging 53 546–61

[32] B Benua R S, Cicale N R, Sonenberg M and Rawson R W 1962 The relation of radioiodine dosimetry to results and complications in the treatment of metastatic thyroid cancer Am. J. Roentgenol. Radium Ther. Nucl. Med. 87 171–82

[33] Benua R S and Leeper R D 1986 A method and rationale for treatment of thyroid carcinoma with the largest, safe dose of 131-I Frontiers in Thyroidology ed G Medeiros-Neto and E Gaitan (New York: Plenum Medical) p 1317

Momennezhad M1, Nasseri S2, Zakavi SR3, Parach AA4, Ghorbani M1, Asl RG1 A 3D Monte Carlo Method for Estimation of Patient-specific Internal Organs Absorbed Dose for (99m)Tc-hynic-Tyr(3) octreotide Imaging. World J Nucl Med. 2016 May-Aug;15(2):114-23.